RSC Advances

This is an *Accepted Manuscript*, which has been through the Royal Society of Chemistry peer review process and has been accepted for publication.

Accepted Manuscripts are published online shortly after acceptance, before technical editing, formatting and proof reading. Using this free service, authors can make their results available to the community, in citable form, before we publish the edited article. This *Accepted Manuscript* will be replaced by the edited, formatted and paginated article as soon as this is available.

You can find more information about *Accepted Manuscripts* in the Information for Authors.

Please note that technical editing may introduce minor changes to the text and/or graphics, which may alter content. The journal's standard Terms & Conditions and the Ethical guidelines still apply. In no event shall the Royal Society of Chemistry be held responsible for any errors or omissions in this *Accepted Manuscript* or any consequences arising from the use of any information it contains.

ROYAL SOCIETY OF CHEMISTRY

www.rsc.org/advances

Journal Name RSCPublishing

ARTICLE

Synthesis of polypyrrole-titanium dioxide brush-like nanocomposites with enhanced supercapacitive performance

Cite this: DOI: 10.1039/x0xx00000x

Received 00th January 2012,
Accepted 00th January 2012

DOI: 10.1039/x0xx00000x

www.rsc.org/

Yan Gao,† Yanzhou Wang,† Xin Xu,* Kun Ding and Demei Yu*

In this work, a kind of polypyrrole (PPy) layer-PPy nanowire-TiO_2 nanotube brush-like composite has been successfully prepared. Highly ordered and free-standing TiO_2 nanotube arrays were prefabricated via an anodizing method, pyrrole was then filled and polymerized in the nanotube arrays through an electrochemical deposition route to form a nanowire-in-tube structure together with a PPy layer outside. The morphology of the as-prepared hybrid nanostructure was observed by scanning electron microscope (SEM), the PPy filling in the TiO_2 nanotube was confirmed by Fourier transform infrared spectroscopy (FTIR) and Raman spectroscopy. When investigated as an anode material for supercapacitors, the as-obtained PPy/TiO_2 could deliver a capacity of 446 F g^{-1} at a current density of 15 A g^{-1} even after 1000 cycles, which is much higher than individual TiO_2 nanotubes and PPy, respectively. The smart nanostructure of the PPy/TiO_2 nanocomposites makes a prominent contribution to the excellent electrochemical performance.

1. Introduction

Electrochemical supercapacitors have attracted massive attention on account of their considerable power density and high specific capacitance in energy storage field.[1-3] Due to the electrochemical performance of supercapacitors is mainly depends on the property of the electrode materials,[4-6] researchers are focused on finding acceptable substitute for traditional electrode materials. The general electrode materials can be classified as carbon materials,[7-9] transition metal oxides[10-12] and conducting polymers.[13-15] In the past few decades, carbon materials such as carbon NWs,[16] carbon nanotubes (CNTs),[17-19] and graphene[20-22] have been intensely investigated as electrode materials, however, the relatively lower power density and specific capacitance extremely limited their practical application.[23] Recently, transition metal oxides and conducting polymers have attracted numerous attentions due to their high Faraday pseudocapacitance. However, their primary limitation is the inferior cycling stability which is mainly originated from the large polarization of the electrode materials during the charge-discharge processes.[24,25] To overcome the problems mentioned above, one promising way is to design and fabricate the conducting polymer-transition metal oxide nanocomposites to enhance their structural stability.[26,27]

Among various pseudocapacitive materials, PPy has attracted much attention on account of its electrochemical reversibility, good conductivity and environmental friendly.[28-30] In recent years, multifarious PPy nanostructures have been developed as electrode materials for supercapacitors and thus obtained remarkable cycling stability.[29,31,32] However, the composite often need intricate synthesis conditions. For example, Hashmi et al[33] have reported the composites of PPy and manganese dioxide, but the monomer pyrrole and β-MnO_2 need to be electrochemical deposited on Indium Tin Oxide (ITO) coaled glass substrate with stirring. Juan Li's[34] strategy to design a MnO_2/PPy composite for electrochemical capacitor need an oxidizing reaction with stirring under static condition for 24 h at the specific temperature of -5 to 0°C. Sivakkumar et al[35] prepared a ternary composite of CNT/polypyrrole/hydrous MnO_2 by in situ chemical method for electrochemical capacitors, but their strategy need sonication pretreatment and have strict requirements for temperature. Therefore, it is

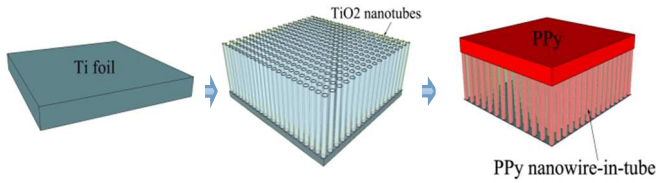

Scheme 1. Schemetic diagram showing the preparation of PPy/TiO2 nanocomposites.

RSC Advances Accepted Manuscript

particularly important to look for a general and facile method to get PPy-transition metal oxide composites. TiO_2 nanotube is one of the important materials for photocatalysis,[36] gas sensing,[37] dye-sensitized solar cells[38,39] which can be fabricated through anodic oxidation, sol–gel, electrodeposition, hydrothermal synthesis, and template synthesis methods.[40-44] During the several methods, anodic oxidation to prepare titanium dioxide nanotube array has a unique advantage: solution mixed evenly, easy to control, simple operation and so on. The as-prepared TiO_2 nanotube array possesses chemical/electrochemical stability[45] and thus can be used as a proper substrate for preparation of PPy-transition metal oxide composites. The electropolymerization process can be performed directly on TiO_2 nanotube arrays and thus presents a facile way to obtain a PPy/TiO_2 composite.

Herein, a brush-like nanocomposite of PPy-TiO_2 for the electrode material of supercapacitors was prepared by a two-step electrochemical method. Scheme 1 shows the synthetic process of the PPy/TiO_2 composite. Firstly, highly ordered, free-standing TiO_2 nanotube array was prefabricated by an anodization method in a three electrode system. The growth mechanism of TiO2 nanotubes can be summarized as four steps:

$$H_2O \rightarrow 2H^+ + O^{2-} \quad (1)$$

$$Ti - 4e \rightarrow Ti^{4+} \quad (2)$$

$$Ti^{4+} + 2O^{2-} \rightarrow TiO_2 \quad (3)$$

$$TiO_2 + 6F^- + 4H^+ \rightarrow [TiF_6]^{2-} + 2H_2O \quad (4)$$

The first stage is the formation of the oxide film, mainly depends on the content of H_2O, then the oxide layer was eroded by fluorine ion and thus nanotubes were obtained. The morphology of TiO_2 nanotubes can be controlled by the composition of the electrolyte, anodization voltage and anodization time. And then the as-obtained TiO_2 nanotube array was used for the filling and polymerization of pyrrole through an electrochemical deposition method. The PPy layer-PPy nanowire-TiO_2 nanotube brush-like composite is believed to be very suitable as an electrode material for supercapacitors, and at least three reasons can be listed: firstly, nanostructured PPy is conducive to the absorption and reaction of the electrolyte ion; Secondly, the TiO_2 nanotube array provides a limited space, which can reduce the volume variation of the intimal PPy during the charge-discharge progress, leading to a favorable cycling stability of the TiO_2 based nanocomposite. Lastly, the stable TiO_2 is used as template and PPy with high capacity can be deposited in the template, the stabiliy of the TiO_2 template and the high capacity of the PPy generates synergies and promotes the utilization of active materials.

2. Experimental Section

2.1 Material Synthesis

TiO_2 nanotube array: The TiO_2 nanotube array was prepared from titanium plate using an anodizing method in organic solution according to the procedure introduced in Refs.[42] The titanium plate was grinded and polished into sheet (30 mm × 30 mm × 0.5 mm), then applied into ultrasonic cleaning in acetone, ethanol and deionized water every 10 minutes. Then, a potentiostatic anodization process was adopted at 30 V for 8 h in an ethylene glycol solution containing 0.5% mass fraction ammonium fluoride, 2% volume fraction deionized water using titanium plate as anode and Pt for cathode. Through washing and drying, a layer of amorphous titanium dioxide nanotube film was obtained.

PPy/TiO_2 composites: PPy/TiO_2 nanotube hybrid was prepared through an electrochemical synthesis route on PAR-2273 type electrochemical workstation. A normal constant voltammetry deposition method was adopted to prepare PPy/TiO_2 nanotube hybrid in a three-electrode system using TiO_2/Ti as a working electrode, Pt as a counter electrode and silver electrode as a reference electrode in an organic acetonitrile solution containing 0.2 M polypyrrole and 0.1 M lithium perchlorate ($LiClO_4$) supporting electrolyte. Polymerization was applied under constant voltage of 0.8 V for 5-30 min. As-formed PPy/TiO_2 was repeatedly washed with deionized water and finally dried at room temperature.

2.2 Characterization

The surface morphology and microstructure of TiO_2 nanotube array and PPy/TiO_2 nanocomposites were investigated using scan electron microscopy (SEM). To identify the chemical structure of TiO_2 nanotube array and PPy/TiO_2 nanocomposites, infrared spectroscopy was performed using fourier transform infrared spectrometer (FTIR) in the range of 400–4000 cm^{-1} and Raman spectroscopy was performed using Raman spectrometer in the range of 100-3000 cm^{-1}.

2.3 Electrochemical measurements

The composites for fabricating electrode were prepared by mixing active materials (70 wt%), carbon black conductive agent(20 wt%), and polytetrafluoroethylene binder(10 wt%) together. Then the mixture was diluted with a small amount of NMP and stirred at 25 °C for 24 h to be mixed thoroughly. The materials were then coated on the surface of carbon foam (1 cm × 2 cm), dried at 60 °C for 8 h, and dried in vacuum at 140 °C for 8 h to get PPy/TiO_2 electrode. All electrochemical measurements were carried out in a conventional three-electrode system with a platinum counter electrode and a standard calomel reference electrode (SCE) and PPy/TiO_2 composite working electrode. The electrolyte was 1 M H_2SO_4. The cyclic voltammetry measurement was carried out using an electrochemical workstation (CHI660D) in 1 M H_2SO_4 electrolyte solution. The supercapacitive behaviors of the composite electrode were evaluated by galvanostatic charge/discharge tests with electrochemical workstation (CHI660D) at room temperature. The galvanostatic charge/discharge test was conducted under different current density with potential window range of 0-1 V. The EIS

RSC Advances Accepted Manuscript

This journal is © The Royal Society of Chemistry 2012

measurement was performed with electrochemical workstation (CHI660D) at open-circuit potential with frequency in the range of 0.1 Hz-100 kHz.

3. Results and discussion

The TiO_2 nanotube array with highly ordered and free-standing structures was prepared through an anodization process. Then pyrrole was deposited and polymerized in the TiO_2 nanotubes and on the surface of TiO_2 nanotube array to form brush-like PPy structure. Thus a kind of brush-like PPy and coaxial TiO_2 nanotube hybrid structure was obtained. SEM images of TiO_2 nanotube array are shown in Fig. 1. It can be seen that the free-standing TiO_2 nanotubes were successfully fabricated, and these orderly nanotubes are separated from each other. From the top-section and cross-section view it can be seen clearly that the TiO_2 nanotube is about 4200 nm in length and about 50-70 nm in diameter. In addition, the individual TiO_2 nanotube is open on the top, closed at the bottom and possesses a tube wall thickness in the range of 10–20 nm. Meantime, the tube length of the TiO_2 nanotube array can be controlled by anodization time, as shown in Fig. S1. The length of the TiO_2 nanotubes will increase over time within a range of 2-8 h. When the anodization time is more than 8 h, the tube length almost remain unchanged, as the growth and the dissolution of the oxide layer reached a balance. The highly ordered and vertically oriented TiO_2 nanotube array offers a high surface area. Such an independent and tubular nanostructure is beneficial for polypyrrole to embed.

SEM images of PPy/TiO_2 nanocomposites are shown in Fig. 2. We can see the PPy/TiO_2 nanocomposite exhibit an ordered and heterogeneous coaxial nanostructure. The pyrrole can be easily deposited and encapsulated in the TiO_2 nanotubes to form PPy nanowires, because the highly ordered TiO_2 nanotube array offers a high surface area which is helpful to fill the TiO_2 nanotube with polypyrrole. Fig. 2a shows the brush-like structure of the PPy/TiO_2 composite. As can be seen, the PPy layer is about 1.2 μm thickness and TiO_2 nanotubes are about 5.3 μm in length. To investigate the PPy nanowire-in-TiO_2 nanotube structure, we peeled of the PPy layer and followed a magnified observation. It can be seen clearly that the PPy nanowires are formed inside of the TiO_2 nanotubes (Fig. 2b). The PPy nanowires can be observed clearly in Fig. 2c

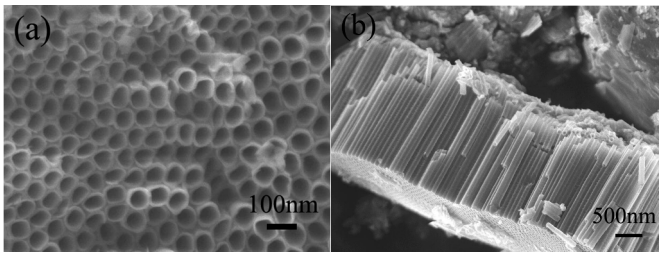

Fig. 1 SEM images of TiO_2 nanotube arrays. (a) Top surface view, (b) cross-section view.

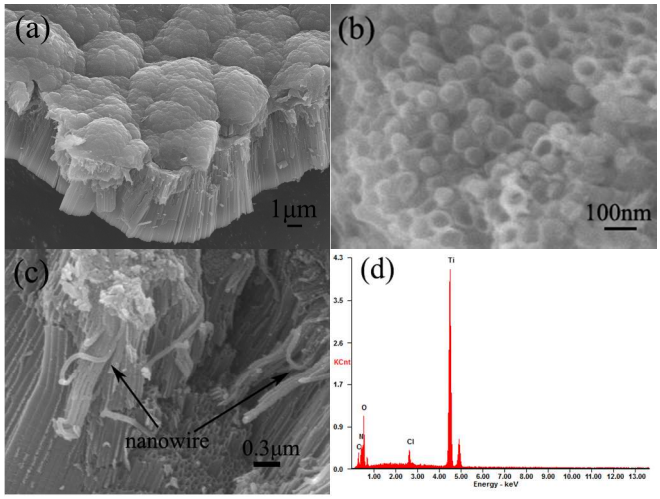

Fig. 2 SEM images of PPy/TiO_2 nanocomposites and PPy nanowires. (a, b) top surface view and cross-section view of PPy/TiO_2 nanocomposites, (c) PPy nanowires stretched out of TiO_2 nanotubes, (d) EDX spectra of PPy/TiO_2 nanocomposites.

in the fracture section of the composite. During the peeling off process, part of the PPy nanowires were separated from the TiO_2 nanotubes. The PPy nanowires are about 70 nm in diameter and 1.5 μm in length. It is thus evident that the controlled electropolymerization process is a feasible approach to form the brush-like PPy/TiO_2 hybrid structure. It is thought that the brush-like structure contributes highly effective interface area to shorten the ion diffusion path and electron transfer path, consequently improving the electrochemical capacitance performance. To further investigate the brush-like structure of PPy/TiO_2 composites, the energy dispersive X-ray (EDX) analysis was carried out. As shown in Fig. 2d, the EDX spectrum of the composites shows strong Kα and Kβ diffraction peaks from Ti element appearing at 4.51 and 4.92 keV; the peak of O element is at 0.533 keV; at the same time, 0.276 keV and 0.397 keV diffraction peaks correspond to the elements of C and N elements. The appearance of Cl element is due to the electrolyte used in electrochemical deposition containing $LiClO_4$. The mass distribution of each element is shown in Table 1.

The FTIR spectra of PPy and the PPy/TiO_2 composites are presented in Fig. 3. From the infrared spectrogram of chemical synthetic PPy (II), all characteristic peaks of PPy can be observed. N-H stretching vibration peak was shown at 3417 cm^{-1}. The peaks at 1450 cm^{-1} and 1539 cm^{-1} correspond to pyrrole ring C=C and C-N stretching vibration. The peaks at 1033 cm^{-1} and 1116 cm^{-1} belong to the deformation of N-H and vibration of C-H, respectively; the peaks at 775 cm^{-1} and 900 cm^{-1}

Table 1
Elements content of PPy/TiO_2 composites.

Element	C	N	O	Cl	Ti
Wt (%)	4.74	7.3	34.24	1.86	51.86

RSC Advances Accepted Manuscript

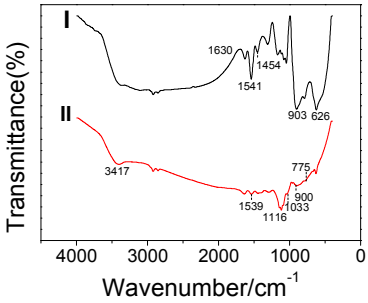

Fig. 3 FTIR spectra of PPy/TiO_2 nanocomposites (I) and chemical synthetic PPy (II).

correspond to the C-H swing vibration. Meantime, the characteristic peaks of PPy can also be observed in infrared spectrum of PPy/TiO_2 composites. From infrared spectrum of PPy/TiO_2 composites shown in Fig. 3 (I), we can see characteristic peaks of C=C at 1630 cm^{-1}, 1541 cm^{-1} and 1454 cm^{-1} is ascribed to C-N stretching vibration peak. The peak at 903 cm^{-1} accounts for C-H swing vibration. The absorption peak at 626 cm^{-1} is attributed to the characteristic peak of Ti-O, which proves the existence of TiO_2. The main characteristic peaks of PPy can be found both at the infrared spectrum of the composites and that of PPy, and the characteristic peak of TiO_2 is observed in the spectrum of the composite, thus the co-existence of TiO_2 and PPy is proved.

The Raman spectra of PPy/TiO_2 brush-like composites are shown in Fig. 4. Regarding the Raman spectra of the composites under the low energy light, characteristic absorption peaks of PPy can be found. The absorption peak at 1582 cm^{-1} is ascribed to C=C stretching vibration. The absorption peaks at 1372 cm^{-1} and 1332 cm^{-1} correspond to C-C and C-N stretching vibration, respectively. The absorption peak at 1227 cm^{-1} is ascribed to C-H in-plane bending vibration. The absorption peaks at 1077 cm^{-1} and 930 cm^{-1} are because C-H ring deformation vibration. When the composite was irradiated with high-energy light, characteristic absorption peaks of TiO_2 can be observed. The peaks at around 153 and 630 cm^{-1} are ascribed to O-Ti-O symmetric deformation vibration and Ti-O stretching vibration, respectively. It is believed that under high-energy light, PPy was resolved

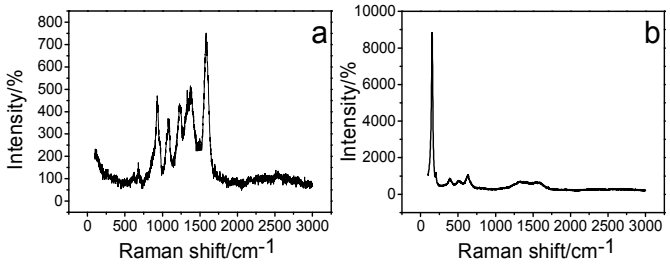

Fig. 4 Raman spectra of PPy/TiO_2 nanocomposites. (a) under low energy light, (b) under high energy light.

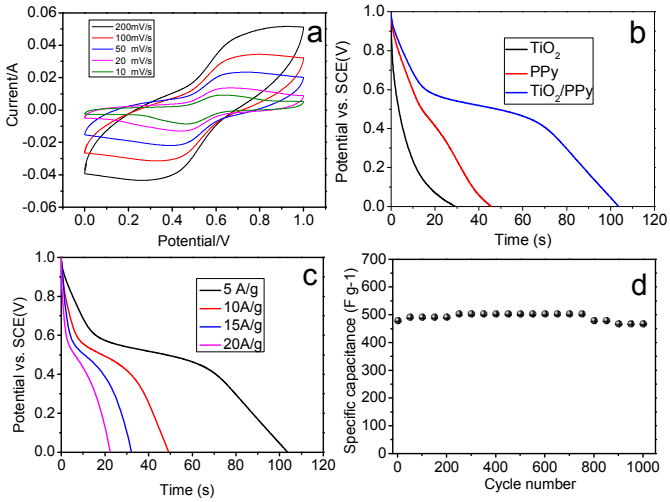

Fig. 5 (a) CV curves of PPy/TiO_2 composite at scan rates from 10 mV s^{-1} to 200 mV s^{-1}. (B) Galvanostatic charge/discharge curves of TiO_2, PPy and PPy/TiO_2 composites at the current density of 5 A g^{-1}. (C) Specific capacitances of PPy/TiO_2 composites at current densities of 5 A g^{-1}, 10 A g^{-1}, 15 A g^{-1} and 20 A g^{-1}. (D) Cycle life of the PPy/TiO_2 composites at the current density of 15 A g^{-1}.

and the absorption peak of TiO_2 can be observed.The characteristic peaks of PPy and TiO_2 have proven the formation of PPy/TiO_2 nanocomposite through an electrodeposition process.

Fig. 5a shows the cyclic voltammetry (CV) curves of PPy/TiO_2 composite measured in the electrolyte of 1 M H_2SO_4 at scan rates from 10 mV s^{-1} to 200 mV s^{-1}. It reveals an oblique and narrow CV loop, reflecting the pseudocapacitive characteristic of the conducting polymers. Fig. 5b shows galvanostatic discharge curves of the TiO_2, PPy and PPy/TiO_2 composites at a current density of 5 A g^{-1}. The gravimetric specific capacitance (Cm) is calculated using the following equation:

$$C_m = I \times \Delta t / (\Delta V \times m)$$

where C_m (F g^{-1}) is the specific capacitance, I (A) is the discharge current, Δt (s) is the discharge time, ΔV (V) is the potential change during discharge, and m (g) is the mass of the active material (PPy/TiO_2 composites) in each electrode. Under the same condition of 5 A g^{-1} current density, the storage capacity of titanium dioxide, polypyrrole, and PPy/TiO_2 composite materials are 146 F g^{-1}, 228 F g^{-1} and 518 F g^{-1}. In addition, the specific capacitances of the PPy/TiO_2 composite at different current densities are also measured subsequently with the results shown in Fig. 5c. The potential plateau at around 0.5–0.6 V appears in the discharge curve at a current density of 5 A g^{-1}, corresponding to the Faradaic discharge process. With the increasement of the current density, the discharge potential plateaus are weakened gradually and almost disappear at the current density of 20 A g^{-1}. Under different current density, the composite material discharge capacitance is also different.

RSC Advances Accepted Manuscript

This journal is © The Royal Society of Chemistry 2012

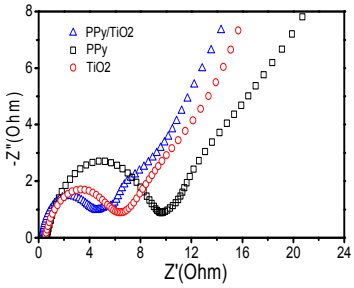

Fig. 6 Nyquist plots of TiO_2, PPy, and PPy/TiO_2 composite at open circuit potential.

Corresponding to 5 A g^{-1}, 10 A g^{-1}, 15 A g^{-1}, 20 A g^{-1}, the discharge capacitance were 518 F g^{-1}, 491F g^{-1}, 480 F g^{-1} and 446 F g^{-1}, respectively. The specific energy density (E) and power density (P) can be calculated according to the following equations:

$$E= C_m\times\Delta V^2/2,\ P=I\times\Delta V/2m$$

Where C_m is the specific capacitance, E is the energy density, P is the power density, I is the discharge current, Δt is the discharge time, ΔV is the potential window, and m is the mass of the active material. The specific energy density and power density of PPy/TiO_2 composite under the current density of 15 A g^{-1} are accordingly caculated to be 240 Wh kg^{-1} and 7.5 Wh kg^{-1}, respectively. The cycling stability of PPy/TiO_2 composite is displayed in Fig. 5d. When the charge–discharge current density is 15 A g^{-1}, the specific capacitance of the PPy/TiO_2 nanocomposite is 480F g^{-1}, at the end of 1000 cycles, leading to only 7.08% capacity loss. The result reveals that the PPy/TiO_2 nanocomposite has high capacity and excellent cycling stability. The relationship between the length of TiO_2 nanotube arrays and the capacitance of the PPy/TiO_2 nanocomposite was also studied, as shown in Fig. S2. It is clear that the PPy/TiO_2 nanocomposite with longer nanotube length exhibits higher specific capacitance. To make a further comparison, the specific capacitances of the calcined and uncalcined TiO_2 based products were shown in Fig. S3. The calcined TiO_2 based composite exhibited a close specific capacitance of 468 F g^{-1} compared with the calcined TiO_2 based composite (480 F g^{-1}). The unique brush-like structure makes the composite exhibit a higher specific capacitance of 480 F g^{-1} than other TiO_2/PPy combinitions, such as TiO_2@PPy core-shell nanowires (64.6 mF cm^{-2})[32] and PPy-TiO_2 nanotube hybrid in which PPy is loaded onto TiO_2 nanotube walls (382 F g^{-1}).[46]

In addition, the Nyquist spectroscopy was conducted to further analyze the impedance properties of the PPy/TiO_2 nanocomposite as shown in Fig. 6. The PPy/TiO_2 electrode shows the least diameter of a semicircle, indicating a better electrical conductivity than PPy electrode and TiO_2 electrode. The improved supercapacitive property of the PPy/TiO_2 nanocomposite is mainly caused by the synergistic effect between TiO_2 and PPy. Therefore, the composite electrode shows great electrochemical performance and exhibits very high specific capacitance.

Conclusions

A proper material for supercapacitors, PPy/TiO_2 composites with a brush-like structure have been prepared via an electrochemical route. The as-prepared PPy/TiO_2 composites reveal higher discharge capacitance and better cycling performance than single PPy and TiO_2, which could show a capacity of 446 F g^{-1} at a current density of 15 A g^{-1} even after 1000 cycles. It is notable that the wire-in-tube architecture can effectively enhance the capacitance and cycle life of conductive polymer. The TiO_2 nanotubes limitied the volume variation and enhanced the electrochemical performance of high-capacity PPy by offering a stable template. The prepared PPy/TiO_2 nanocomposite exhibits a good synergistic effect of high capacity and strong stability, making the composite a promising material for electrode for supercapacitors.

Acknowledgements

The work was supported by NSFC Major Research Plan on Nanomanufacturing (Grant No. 91323303）

Notes and references

Department of Applied Chemistry, School of Science, Xi'an Jiaotong University, Xi'an 710049, China.
E-mail: xu.xin@stu.xjtu.edu.cn; dmyu@mail.xjtu.edu.cn
†Yan Gao and Yanzhou Wang contributed equally to this work.

1 A. S. Arico, P. Bruce, B. Scrosati, J. M. Tarascon and W. Van Schalkwijk, *Nature Mater.*, 2005, **4**, 366-377.
2 B. E. Conway, *J. Electrochem. Soc.*, 1991, **138**, 1539-1548.
3 R. Kotz and M. Carlen, *Electrochim. Acta*, 2000, **45**, 2483-2498.
4 P. Simon and Y. Gogotsi, *Nature Mater.*, 2008, **7**, 845-854.
5 G. Wang, L. Zhang and J. Zhang, *Chem. Soc. Rev.*, 2012, **41**, 797-828.
6 Y. Zhang, H. Feng, X. Wu, L. Wang, A. Zhang, T. Xia, H. Dong, X. Li and L. Zhang, *Int. J. Hydrogen Energy*, 2009, **34**, 4889-4899.
7 E. Frackowiak and F. Beguin, *Carbon*, 2001, **39**, 937-950.
8 M. Inagaki, H. Konno and O. Tanaike, *J. Power Sources*, 2010, **195**, 7880-7903.
9 S. Bose, T. Kuila, A. K. Mishra, R. Rajasekar, N. H. Kim and J. H. Lee, *J. Mater. Chem.*, 2012, **22**, 767-784.
10 K. Kuratani, T. Kiyobayashi and N. Kuriyama, *J. Power Sources*, 2009, **189**, 1284-1291.
11 X. Lu, G. Wang, T. Zhai, M. Yu, J. Gan, Y. Tong and Y. Li, *Nano Lett.*, 2012, **12**, 1690-1696.
12 X. Zhang, J. Ma, W. Yang, Z. Gao, J. Wang, Q. Liu, J. Liu and X. Jing, *CrystEngComm*, 2014, **16**, 4016-4022.
13 D. P. Dubal, S. V. Patil, A. D. Jagadale and C. D. Lokhande, *J. Alloys Compd.*, 2011, **509**, 8183-8188.
14 M. Mastragostino, C. Arbizzani and F. Soavi, *J. Power Sources*, 2001, **97-8**, 812-815.
15 D. P. Dubal, S. H. Lee, J. G. Kim, W. B. Kim and C. D. Lokhande, *J. Mater. Chem.*, 2012, **22**, 3044-3052.
16 D.-s. Yuan, T.-x. Zhou, S.-l. Zhou, W.-j. Zou, S.-s. Mo and N.-n. Xia, *Electrochem. Commun.*, 2011, **13**, 242-246.

RSC Advances Accepted Manuscript

17 G. Y. Han, J. Y. Yuan, G. Q. Shi and F. Wei, *Thin Solid Films*, 2005, **474**, 64-69.
18 M. Kaempgen, C. K. Chan, J. Ma, Y. Cui and G. Gruner, *Nano Lett.*, 2009, **9**, 1872-1876.
19 J. Wang, Y. Xu, X. Chen and X. Sun, *Compos. Sci. Technol.*, 2007, **67**, 2981-2985.
20 J. Li and H. Xie, *Mater.Lett.*, 2012, **78**, 106-109.
21 Y. Liu, Y. Zhang, G. Ma, Z. Wang, K. Liu and H. Liu, *Electrochim. Acta*, 2013, **88**, 519-525.
22 L. Van Hoang, T. Huynh Ngoc, H. Le Thuy, H. Nguyen Thi Minh, E.-S. Oh, J. Chung, E. J. Kim, W. M. Choi, B.-S. Kong and S. H. Hur, *J. Mater. Chem. A*, 2013, **1**, 208-211.
23 L. L. Zhang and X. S. Zhao, *Chem. Soc. Rev.*, 2009, **38**, 2520-2531.
24 S. C. Huang, S. M. Huang, H. Ng and R. B. Kaner, *Synth. Met.*, 1993, **57**, 4047-4052.
25 B. C. Kim, J. S. Kwon, J. M. Ko, J. H. Park, C. O. Too and G. G. Wallace, *Synth. Met.*, 2010, **160**, 94-98.
26 J. Duay, E. Gillette, R. Liu and S. B. Lee, *Phys. Chem. Chem. Phys.*, 2012, **14**, 3329-3337.
27 Y. Liu, B. Zhang, Y. Yang, Z. Chang, Z. Wen and Y. Wu, *J. Mater. Chem. A*, 2013, **1**, 13582-13587.
28 H. An, Y. Wang, X. Wang, L. Zheng, X. Wang, L. Yi, L. Bai and X. Zhang, *J. Power Sources*, 2010, **195**, 6964-6969.
29 Y. Xie and H. Du, *J. Solid State Electrochem.*, 2012, **16**, 2683-2689.
30 R. Sharma, A. Rastogi and S. Desu, *Electrochem. Commun.*, 2008, **10**, 268-272.
31 A. Singh, Z. Salmi, N. Joshi, P. Jha, P. Decorse, H. Lecoq, S. Lau-Truong, M. Jouini, D. K. Aswal and M. M. Chehimi, *RSC Advances*, 2013, **3**, 24567-24575.
32 M. Yu, Y. Zeng, C. Zhang, X. Lu, C. Zeng, C. Yao, Y. Yang and Y. Tong, *Nanoscale*, 2013, **5**, 10806-10810.
33 S. A. Hashmi and H. M. Upadhyaya, *Ionics*, 2002, **8**, 272-277.
34 J. Li, L. Cui and X. Zhang, *Appl. Surf. Sci.*, 2010, **256**, 4339-4343.
35 S. R. Sivakkumar, J. M. Ko, D. Y. Kim, B. C. Kim and G. G. Wallace, *Electrochim. Acta*, 2007, **52**, 7377-7385.
36 Q. Luo, X. Li, D. Wang, Y. Wang and J. An, *J. Mater. Sci.*, 2010, **46**, 1646-1654.
37 R. Lu, W. Zhou, K. Shi, Y. Yang, L. Wang, K. Pan, C. Tian, Z. Ren and H. Fu, *Nanoscale*, 2013, **5**, 8569-8576.
38 Y. Hou, X. Li, Q. Zhao, X. Quan and G. Chen, *J. Mater. Chem.*, 2011, **21**, 18067-18076.
39 J. Akilavasan, K. Wijeratne, H. Moutinho, M. Al-Jassim, A. R. M. Alamoud, R. M. G. Rajapakse and J. Bandara, *J. Mater. Chem. A*, 2013, **1**, 5377-5385.
40 D. Li and Y. N. Xia, *Nano Lett.*, 2003, **3**, 555-560.
41 N. Liu, X. Chen, J. Zhang and J. W. Schwank, *Catal. Today*, 2014, **225**, 34-51.
42 G. K. Mor, O. K. Varghese, M. Paulose, K. Shankar and C. A. Grimes, *Sol. Energy Mater. Sol. Cells*, 2006, **90**, 2011-2075.
43 Y. Jo, I. Jung, I. Lee, J. Choi and Y. Tak, *Electrochem. Commun.*, 2010, **12**, 616-619.
44 J. Lin, J. Chen and X. Chen, *Electrochem. Commun.*, 2010, **12**, 1062-1065.
45 X. Xu, Z. Fan, S. Ding, D. Yu and Y. Du, *Nanoscale*, 2014, **6**, 5245-5250.
46 H. Du, Y. Xie, C. Xia, W. Wang and F. Tian, *New J. Chem.*, 2014, **38**, 1284-1293.

RSC Advances Accepted Manuscript

This journal is © The Royal Society of Chemistry 2012

Graphical Abstract

Polypyrrole-titanium dioxide brush-like nanocomposites show enhanced electrochemical performance and excellent cycling stability as an electrode material for supercapacitors.

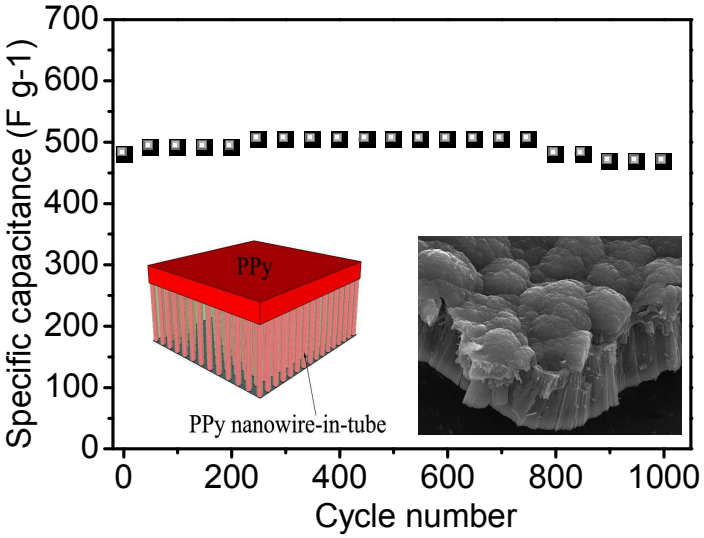

RSC Advances Accepted Manuscript